Journal of Hard Tissue Biology 27[4] (2018) 343-350

CODEN-JHTBFF, ISSN 1341-7649

Original

Bone Morphogenetic Protein-2 Accelerates Osteogenic Differentiation in Spheroid-Derived Mesenchymal Stem Cells

Naoyuki Miyaguchi[1,2], Hiroshi Kajiya[2,3], Masahiro Yamaguchi[2,4], Ayako Sato[1,2], Madoka Yasunaga[2,5], Takuya Toshimitu[2,6], Tsukasa Yanagi[1,2], Ayako Matsumoto[1,2], Hirofumi Kido[1] and Jun Ohno[2]

[1] *Section of Oral Implantology, Department of Oral Rehabilitation, Fukuoka Dental College, Fukuoka, Japan*
[2] *Research Center for Regenerative Medicine, Fukuoka Dental College, Fukuoka, Japan*
[3] *Section of Cellular Physiology, Department of Physiological Science and Molecular Biology, Fukuoka Dental College, Fukuoka, Japan*
[4] *Section of Geriatric Dentistry, Department of General Dentistry, Fukuoka Dental College, Fukuoka, Japan*
[5] *Section of Orthodontics, Department of Oral Growth and Development, Fukuoka Dental College, Fukuoka, Japan*
[6] *Dentistry for the Disabled, Department of Oral Growth and Development, Fukuoka Dental College, Fukuoka, Japan*
(Accepted for publication, September 8, 2018)

Abstract: Spheroid culture systems more accurately recreate the *in vivo* microenvironment and are susceptible to factors that induce differentiation. In this study, we assessed whether bone morphogenetic protein (BMP)-2 induces enhanced osteogenic differentiation in spheroid-derived mesenchymal stem cells (MSCs). MSC spheroids were generated from human adipose tissue-derived MSCs using low-binding plates. Osteogenic differentiation of monolayer and spheroid-derived MSCs was induced by osteogenesis induction medium (OIM) with or without BMP-2. Increased alkaline phosphatase and Alizarin Red staining were observed in spheroid-derived MSCs treated with a mixture of OIM and BMP-2, compared with monolayer MSCs. Spheroid-derived MSCs had increased mRNA and protein expressions of osteogenic runt-related transcription factor 2 (Runx2) and osterix (OSX). The intranuclear expression of OSX was also observed in spheroid-derived MSCs treated with the mixture of OIM and BMP-2. In addition, spheroid-derived MSCs with BMP-2 treatment showed the upregulation of Smad5 mRNA and phosphorylated Smad1/5, suggesting that the Smad-BMP signaling pathway is enhanced in these cells. Our data indicate that the Smad-dependent BMP signaling pathway accelerates osteogenic differentiation in spheroid-derived MSCs, compared with monolayer MSCs.

Key words: Osteogenesis, Mesenchymal stromal cells, Bone morphogenetic protein 2, Spheroid culture, Smad

Introduction

Adult mesenchymal stem cells (MSCs) are found in pulp, cord blood, umbilical cord and others[1-4]. MSCs possess great potential for tissue engineering and regenerative medicine, because of their capability of self-renewal and multilineage differentiation. MSCs have been utilized as a cell source for osteogenic tissue regeneration because culture in the presence of osteogenic supplements facilitates MSCs to undergo differentiation into the osteogenic phenotypes[5, 6].

Osteogenic differentiation is regulated by various signaling pathways, including Wnt, bone morphogenetic protein (BMP), Hedgehog, Notch, and fibroblast growth factors. BMPs, members of the transforming growth factor-β (TGF- β) superfamily, regulate proliferation, differentiation, and apoptosis in various types of cells and organs in embryonic development and postnatal physiological function[7]. When BMPs-containing scaffolds are implanted into rodent tissues, ectopic bone formation is induced by BMPs. BMPs, including BMP-2 and -4, accelerate osteoblast differentiation of MSCs via activation of transcription factors, such as Runx2/core binding factor a1 (Cbfa1) and Sp7/osterix[8, 9]. In addition, Smad proteins play an important role in the intracellular signaling of BMPs in mammals[9]. Receptor-activated Smad (R-Smad) proteins, Smad1, Smad2, Smad3, Smad5, and Smad8, are directly phosphorylated by type I TGF-β receptors. Upon activation, R-Smad form complexes with the Co-Smad, Smad4, and translocate to the nucleus to regulate gene expression by binding to regulatory regions of the target genes.

Although relatively easy and traditional, 2D culture is an artificial and less physiologically relevant environment, because *in vivo* characteristics and traits are lost or compromised. Furthermore, in conventional 2D *in vitro* monolayer culture techniques, MSCs eventually lose intrinsic properties, such as self-renewal, replication, colony-forming efficiency, and differentiation capacity[10-12]. Spheroid 3D environments are generally considered more favorable than 2D monolayer culture. Various culture systems have recently been developed to generate 3D multicellular spheroids from MSCs, such as suspension, hanging drop, micropattern substrates, and non-adherent surfaces[13-16]. In 3D-cultured spheroids, self-renewal has been reported to be significantly enhanced[17, 18]. Additionally, MSC spheroids formed on micropattern substrates and non-adherent surfaces have higher osteogenic and adipogenic differentiation efficiencies[16, 19]. In this study, we employed a low-attachment culture condition to generate MSC spheroids. The osteogenic properties of spheroid-derived MSCs were investigated. We further examined an effect of BMP-2 on acceleration of osteogenesis in spheroid-derived

Correspondence to: Dr. Jun Ohno, Research Center for Regenerative Medicine, Fukuoka Dental College, 2-15-1 Tamura, Sawara-ku, Fukuoka, Fukuoka 814-0193, Japan; Tel: +81928010411 (Ext 684); Fax: +81928014909; E-mail: johno@college.fdcnet.ac.jp

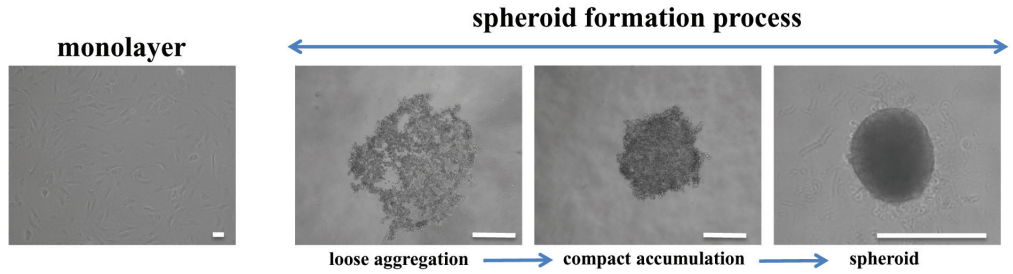

Figure 1. MSC spheroid formation. Representative phase-contrast images showing the process of hMSC spheroid formation. Parental cell line in monolayer culture was used (monolayer, scale bar = 50 μm). During the generation process of MSC spheroids, loose cellular aggregation of MSCs was observed after 2 hours in microplate culture. After the cellular aggregation formed a compact accumulation at 4 hours, a compact spheroid was observed at 24 hours (Scale bars = 500 μm).

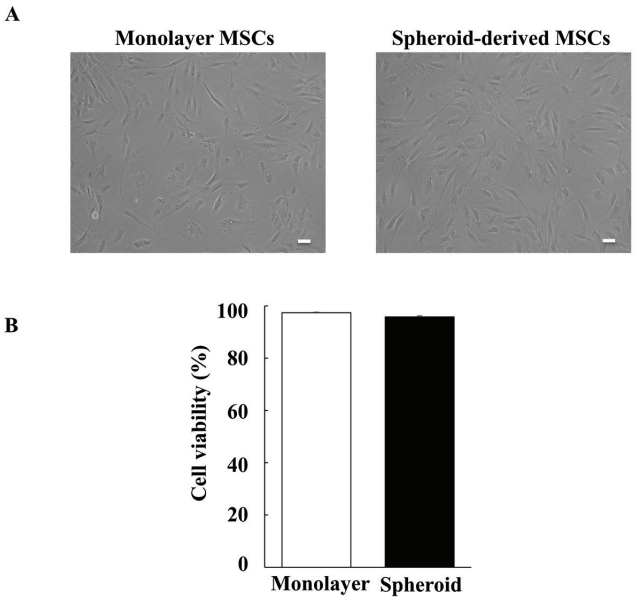

Figure 2. Cell morphology and viability of monolayer- and spheroid-derived MSCs. A: Phase-contrast images of MSCs derived from monolayer and spheroid culture at 24 h after culturing dissociated cells onto dishes. Scale bars, 50 μm. B: Cell viability was determined by trypan blue dye exclusion. All values are presented at the means ± SD from five independent experiments. There are no significant difference between cells derived from monolayer and spheroid culture (Student's t-test).

MSCs. Possible mechanisms for activation of osteogenesis via the BMP pathway are discussed based on spheroid formation of MSCs.

Materials and Methods

MSC monolayer expansion

The human adipose tissue-derived mesenchymal stem cell line HAdpc-25-Bmi-1-TERT was purchased from the Japanese Collection of Research Bioresources Cell Bank (Osaka, Japan). Cryopreserved MSCs were thawed and plated onto a tissue culture dish maintained in complete Poweredby10 expansion medium (GlycoTechnia Ltd., Yokohama, Japan). Cells were dissociated with 0.25% trypsin/EDTA (Invitrogen, Tokyo, Japan), counted, and either re-plated for monolayer cultures or used for spheroid formation.

Spheroid formation of MSCs

Dissociated MSC monolayers were resuspended in complete Poweredby10 expansion medium to obtain a single cell suspension. MSCs (1×10^5 cells/ml, corresponding to approximately 10,000 cells/well) were added to Corning®96 well Ultralow Attachment micro plates (Corning, NY, USA) and incubated in Poweredby 10 expansion medium at 37˚ for 24 h.

Morphology and cell viability of spheroid-derived MSCs

After 24 h of suspension culture, MSC spheroids were washed three times with PBS and incubated with 0.25% trypsin-EDTA solution at 37ºC for 15 min with mechanical agitation until a single-cell suspension was obtained. Dissociated cells were plated and cultured as described above for morphology, cell viability, and differentiation assays. Cell morphology of spheroid-derived MSCs was observed using a phase-contrast microscopy. To determine cell viability, cell suspension of monolayer and spheroid-derived MSCs were diluted 1:1 in 0.4% trypan blue solution (Invitrogen) in PBS. Cell viability was calculated using a Countess Automated Cell Counter (Invitrogen) according to the manufacturer's procedures.

Osteogenic differentiation of monolayer- and spheroid-derived MSCs

For induction of osteogenic differentiation, monolayer- and spheroid-derived cells were seeded and cultured until reaching confluence. The medium was then replaced (Day 0) with osteogenesis-induction medium (OIM) composed of Poweredby 10. Ascorbic Acid (TaKaRa, Tokyo, Japan), hydrocortisone (TaKaRa), β-glycerophosphate (TaKaRa) were added to the medium to 1%, 0.2% and 2%, respectively. The medium was changed every three days for 21 days, with or without 20 ng/ml bone morphologenetic proteins (BMP)-2 (Peprotech, Rocky Hill, NJ, USA).

Alkaline phosphatase (ALP) and Alizarin Red (AR) staining

ALP and AR staining were performed in monolayer and spheroid-derived MSCs treated with or without the experimental solution, using an ALP Kit (Sigma-Aldrich) and Calcified Nodule Staining Kit (Cosmo Bio, Tokyo, Japan), respectively, according to the manufacturer's instructions.

Real-time reverse transcription (RT)-polymerase chain reaction (qRT-PCR)

Total RNA was extracted from monolayer and spheroid-derived cells treated with a mixture of OIM and BMP-2, using ISOGEN reagent (Nippon Gene, Tokyo, Japan). First-strand cDNA was synthesized from total RNA (5 μg) using SuperScript II™ reverse transcriptase (Invitrogen), according to the manufacturer's instructions. The resulting templates were amplified using an Applied Biosystems 7500 Real-Time PCR System (Life Technologies, Carlsbad, CA, USA). Nucleotides,

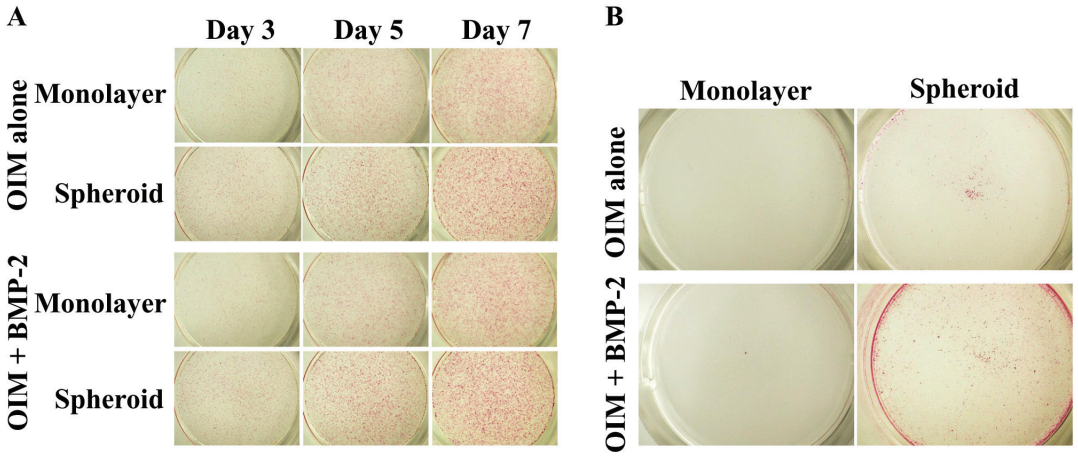

Figure 3. Alkaline phosphatase (ALP) and Alizarin red (AR) staining in monolayer and spheroid-derived MSCs. A: ALP staining was assessed in monolayer- and spheroid-derived cells cultured in the basic medium with OIM alone or a mixture of OIM and BMP-2 (20 ng/ ml) for 3, 5, and 7 days. B: AR staining in monolayer- and spheroid-derived cells treated with OIM alone or a mixture of OIM and BMP-2 (20 ng/ml) for 3 weeks.

TaqDNA polymerase, and a buffer were included in the SYBR Premix Ex Taq II (TaKaRa). β-actin (*ACTB*) was used as an internal control. Relative mRNA expression was normalized as the ratio of runt-related transcription factor 2 (*Runx2*), *Smad5*, or *β-catenin* mRNA to the level of *ACTB* expression. All the reactions were run in hexaplicate. The primers used were *ACTB*, forward 5'-TGGCACCCAGCACAATGAA-3' and reverse, 5'- CTAAGTCATAGTCCGCCTAGAAGCA-3'; *Runx2*, forward 5'-TGTCATGGCGGGTAACGAT-3' and reverse 5'-AAGACGGTTATGGTCAAGGTGAA-3'; *Smad5*, forward 5'-GAGAGTGGAGAGTCCAGTCT-3' and reverse 5'-GGCTGTTTGGAGATAAGGGAAA-3'; *β-catenin*, forward 5'-AGCTGACCAGCTCTCTCTTCA-3' and reverse 5'-CCAATATCAAGTCCAAGATCAGC-3'.

Western blot analysis

Cells were lysed in Cell Lysis Buffer (Cell Signaling Technology, Danvers, MA, USA) containing a 1X Protease/Phosphatase Inhibitor Cocktail (Cell Signaling Technology). Protein samples were loaded and separated onto 4-20% sodium dodecyl sulfate (SDS) polyacrylamide gel, blotted onto PVDF membrane, and incubated with the primary and secondary antibodies. Blots were developed using SignalFire™Plus ECL Reagent (Cell Signaling Technology). The band density was quantified using the NIH-Image J software.

Immunocytochemistry (ICC)

Monolayer- and spheroid-derived MSCs were fixed with 4% paraformaldehyde for 10 min and washed in 0.1% digitonin in phosphate buffered saline (PBS) for 15 min. The cells were incubated with primary antibodies for 2 h at room temperature. After washing with PBS, the cells were incubated with anti-mouse IgG or anti-rabbit IgG conjugated with Alexa Fluor 488 or 568 (Invitrogen) at room for 45 min. To visualize the nuclei, the cells were counterstained with 4', 6-diamidino-2-phenylindole (DAPI; Sigma-Aldrich).

Statistical analysis

Two-way analysis of variance and Holm's multiple comparison test or Student's t-test were used to determine the statistical differences among the samples (StatView for Windows, version 5; SAS Institute, Inc., Cary, CA, USA). Data are presented as the mean ± SD and *P*-values < 0.05 were considered to be statistically significant.

Results

Spheroid formation of hMSCs

First, we examined the generation of spheroids from MSCs in round-bottom, low-binding plates that can generate a single spheroid per well. Spheroid formation was divided into three stages (Fig. 1). Approximately 2 hours after seeding MSC cell into the plates, cells spontaneously and loosely aggregated in the medium. After 4 hours, cellular aggregates began to form a compact accumulation of cells. Finally, cells formed compact multicellular spheroids after 24 hours in suspension culture in low-binding plates.

Cell viability of spheroid-derived MSCs

To observe differences in cell morphology and viability between monolayer- and spheroid-derive MSCs, MSC spheroids were dissociated and seeded back into monolayer culture. Both monolayer- and spheroid-derived MSCs showed spindle and triangular shapes (Fig. 2A). As shown in Fig. 2B, there was no difference in cell viability between monolayer- and spheroid-derived MSCs by trypan blue dye exclusion. Taken together, the dissociation procedure for spheroid-derived MSCs did not affect cell morphology or viability.

A mixture of OIM and BMP-2 accelerates osteogenic differentiation in spheroid-derived MSCs

To investigate the effect of BMP-2 on spheroid-derived MSCs, we first assessed ALP and AR staining in monolayer- or spheroid-derived cells. Figure 3A shows ALP staining in both monolayer and spheroid-derived MSCs cultured in basic medium with OIM alone or a mixture of OIM and BMP-2. ALP staining was evident in spheroid-derived cells on Day 3, even though monolayer cells remained unstained. ALP staining was much more intense in spheroid-derived cells at any time point, compared with monolayer cells. The intensity of ALP staining was significantly enhanced in spheroid-derived cells treated with the mixture of OIM and BMP-2 on Day 7, compared with OIM alone. Three weeks after osteogenic treatment, AR staining showed increased deposition of calcium in spheroid-derived cells treated with the mixture of OIM and BMP-2, compared with other groups (Fig. 3B).

Runx2 and OSX are known to be reliable markers for an early phase of osteogenesis[19-21]. We first used qRT-PCR to examine mRNA expression of *Runx2* in monolayer and spheroid-derived MSCs treated with the

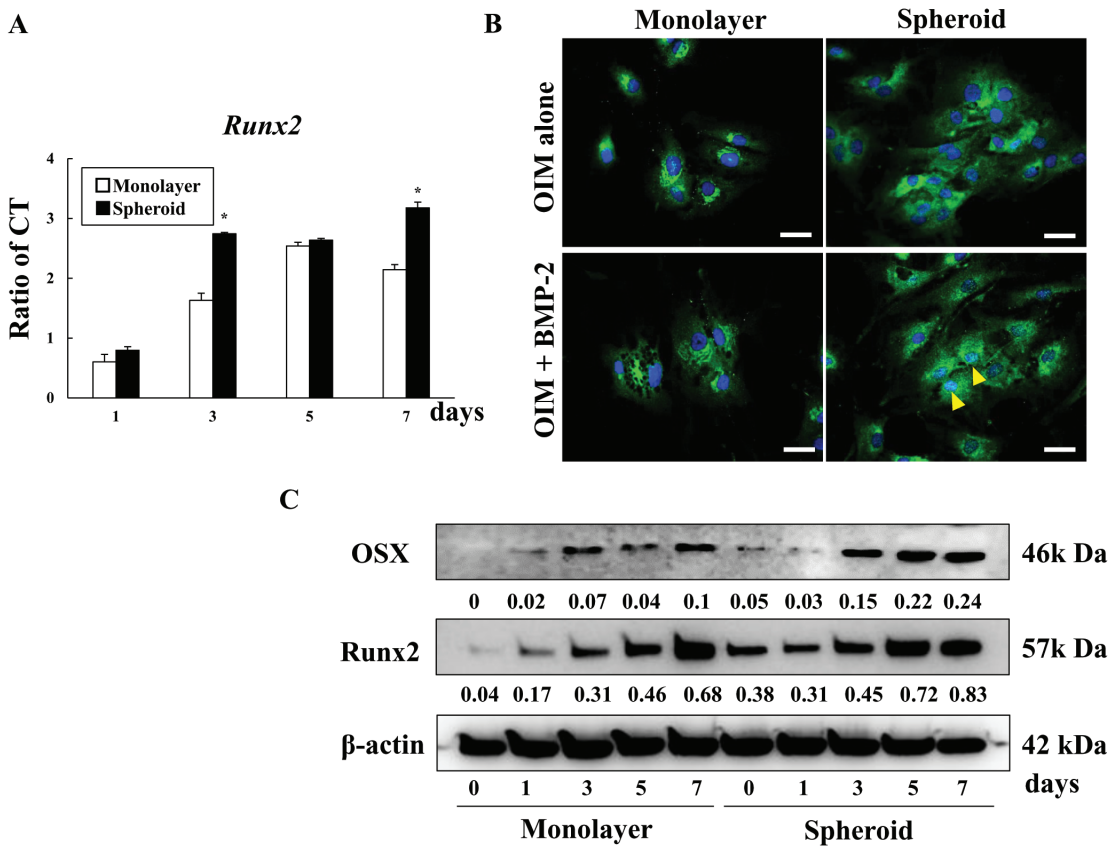

Figure 4. Runx2 and OSX expression in monolayer- and spheroid-derived MSCs. A: Expression of *Runx2* mRNA in monolayer- and spheroid-derived MSCs treated with the mixture of OIM and BMP-2. Data are presented as mRNA expression fold-increases (normalized to *ACTB*) and compared with the results for the monolayer cells treated with the mixture of OIM and BMP-2 on Day 0. Data are presented as the mean ± SD from five cultured wells, each performed at least in triplicate. *, Significantly different at $p < 0.05$ compared with the monolayer cells. B: Immunofluorescence staining of OSX (green) expression in monolayer and spheroid-derived cells treated with OIM alone or the mixture of OIM and BMP-2 (20 ng/ml) on Day 7. Nuclei were stained with 4', 6-diamidino-2-phenylindole (DAPI; blue). Arrowheads, intranuclear expression of OSX. Scale bars = 25 μm. C: Western blot analysis of OSX and Runx2 expression in monolayer- and spheroid-derived cells treated with the mixture of OIM and BMP-2 (20 ng/ml). β-actin was used as a loading control. Bands were quantified with Image J software and values shown represent the fold increase normalize to β-actin.

mixture of OIM and BMP-2 (Fig. 4A). Increased expression of *Runx2* was observed in spheroid-derived MSCs after Day 3. Compared with monolayer-derived MSCs, spheroid-derived cells showed increased expression at all time points, with significant increases on Day 3 and Day 7.

Next, we immunocytochemically examined OSX expression in monolayer- and spheroid-derived MSCs treated with OIM alone or the mixture of OIM and BMP-2 (Fig. 4B). Cytoplasmic expression of OSX was observed in monolayer cells with or without BMP-2 and spheroid-derived cells with OIM alone. In contrast, spheroid-derived cells treated with BMP-2 showed intranuclear expression of OSX in addition to intense cytoplasmic staining.

We then performed western blotting to examine whether expression of osteogenic proteins, such as OSX and Runx2, were upregulated in spheroid-derived MSCs treated with OIM containing BMP-2 (Fig. 4C). Expression of both OSX and Runx2 were upregulated in the spheroid-derived cells treated with OIM containing BMP-2 on Days 3, 5, and 7, compared to monolayer-derived MSCs. These findings indicate that BMP-2 accelerates osteogenic differentiation in spheroid-derived MSCs.

Osteogenesis of spheroid-derived cells is promoted through the BMP signaling pathway

Interactions between the TGF-β/BMP and Wnt/β-catenin signaling pathways play crucial roles in regulation of osteogenesis of MSCs[22]. To elucidate whether both pathways contribute to acceleration of osteogenic induction of spheroid-derived cells, we examined expression of Smads and β-catenin, downstream effectors of BMP and Wnt signaling, respectively, by qRT-PCR, western blotting, and immunocytochemical assays.

Fig. 5A shows the mRNA expression of *Smad 5* and *β-catenin* in monolayer- and spheroid-derived cells treated with the mixture of OIM and BMP-2. *Smad 5* expression was significantly increased in spheroid-derived cells on Day 3 and then decreased to levels similar to Day 1. At all observed time points, *Smad 5* expression was higher in spheroid-derived cells, compared with monolayer cells. In contrast, *β-catenin* mRNA expression gradually increased by Day 7 in both monolayer- and spheroid-derived cells. There were no significant differences in *β-catenin* mRNA expression between monolayer- and spheroid-derived cells at any of the time points.

We next examined whether the expression of phosphorylated Smad 1/5 (p-Smad1/5) and β-catenin proteins were upregulated in monolayer- and spheroid-derived cells treated with the mixture of OIM and BMP-2

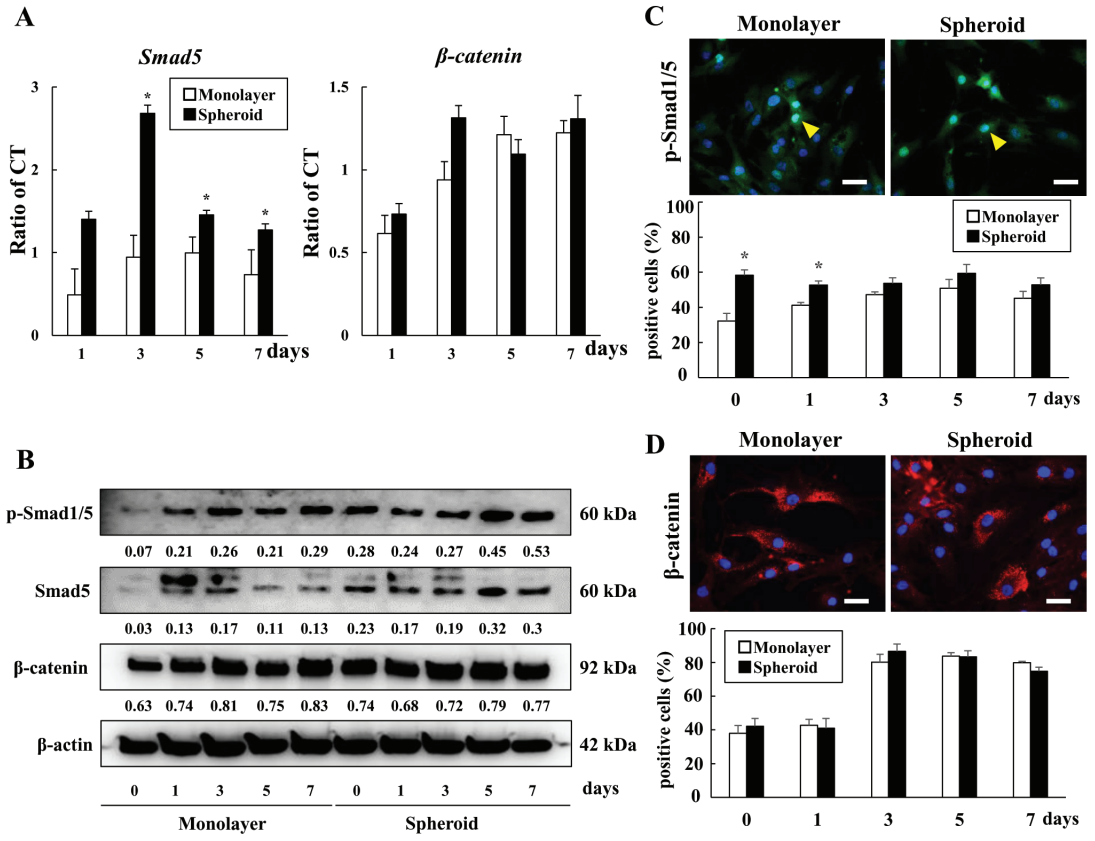

Figure 5. Smad 5 and β-catenin expression in monolayer- and spheroid-derived cells treated with the mixture of OIM and BMP-2. A: qRT-PCR analysis of *Smad 5* and *β-catenin* expression. Results are expressed as the mRNA fold increases (normalized to *ACTB*) and compared with the results for the monolayer cells treated with the mixture of OIM and BMP-2 on Day0. Data shown represent the mean ± SD from five cultured wells, each performed at least in triplicate. *, Significantly different at $p<0.05$ compared with the monolayer cells. B: Western blot analysis of p-Smad1/5, Smad 5, and β-catenin. Bands were quantified with Image J software and values shown represent the fold increase normalized to β-actin (ACTB). Similar results were obtained in five independent experiments. C: Immunofluorescence staining of p-Smad1/5 (green) in monolayer- and spheroid-derived cells treated with the mixture of OIM and BMP-2 on Day 1. Arrowheads, intranuclear expression of p-Smad1/5. Scale bars = 25 μm. A graph shows percentage of p-Smad1/5- or β-catenin-positive cells from monolayer- or sphered-derived cells treated with the mixture of OIM and BMP-2 for 3, 5, and 7 days. Data shown represent the mean ± SD from five cultured slides, each performed at least in triplicate. *, Significantly different at $p<0.05$ compared with the monolayer cells. D: Immunocytochemical expression of β-catenin (red) in monolayer- and spheroid-derived cells treated with the mixture of OIM and BMP-2 on Day 1. Nuclei were stained with DAPI (blue). Scale bars = 25 μm. A graph shows percentage of β-catenin-positive cells from monolayer- or sphered-derived cells treated with the mixture of OIM and BMP-2 for 3, 5, and 7 days. Data shown represent the mean ± SD from five cultured slides, each performed at least in triplicate. *, Significantly different at $p<0.05$ compared with the monolayer cells.

(Fig. 5B). Increased expression of p-Smad 1/5 was observed in spheroid-derived cells, compared with monolayer cells. The relative p-Smad1/5 expression in spheroid-derived cells gradually increased by Day 7. In contrast to p-Smad 1/5 expression, there was no difference in β-catenin expression in either monolayer- or spheroid-derived cells.

Finally, we performed immunocytochemical staining to detect the intranuclear expression of p-Smad 1/5 and β-catenin, because both proteins translocate to the nucleus to initiate downstream gene expression. Intranuclear p-Smad 1/5 expression was significantly upregulated in spheroid-derived cells treated with the mixture of OIM and BMP-2, compared with monolayer cells (Fig. 5C). Incerease in the number of intranuclear p-Smad 1/5-positive cells was observed in spheroid-derived cells at any time points. In contrast, β-catenin expression was localized in the cytoplasm of both monolayer- and spheroid-derived cells treated with the mixture of OIM and BMP-2 (Fig. 5D). There was no difference in the number of cytoplasmic β-catenin-positive cells in monolayer- and spheroid-derived MSCs. These findings suggest that acceleration of osteogenic induction in spheroid-derived cells may be regulated in part through the BMP signaling pathway without dependence on Wnt/β-catenin signaling.

Discussion

Spheroid culture takes advantage the intrinsic self-assembly tendency of numerous cell types allowing cells to adapt native morphology, promoting greater cell-cell contacts and interaction with the extracellular matrix[23]. Our recent study demonstrated that MSC spheroids possess enhanced osteogenic potential, compared with monolayer MSCs[16]. In this study, we present three lines of evidence to support the conclusion that MSC spheroids exhibit enhanced osteogenic potential: (a) spheroid-derived MSCs exhibited increased calcium deposition, compared with monolayer MSCs; (b) expression of osteogenic proteins was upregulated in spheroid-derived MSCs cultured in the mixture of OIM and BMP-2, compared with those in OIM alone or monolayer-derived MSCs treated with the mixture of OIM and BMP-2; (c) osteogenesis of spheroid-derived MSCs was promoted via the BMP signaling pathway.

The round-bottom, low-binding plates used in this study have desir-

able characteristics such as a single spheroid per well, high reproducibility, and simple harvesting for further analysis[24]. In this study, we dissociated MSC spheroids to seed back into monolayer culture for increased permeability of OIM and BMP-2 to whole spheroid-composed MSCs. There were no differences in cell morphology and viability between monolayer-derived MSCs and spheroid-derived MSCs.

OIM-induced osteogenesis in MSCs is characterized by an increase in ALP at early stages, followed by matrix deposition, matrix maturation, and mineralization at later stages[25-27]. BMPs are known to be the most important inducers and stimulators of osteogenic differentiation[8, 9]. In this study, increased staining with ALP was observed in spheroid-derived MSCs cultured in the mixture of OIM and BMP-2. Similarly, AR staining showed matrix mineralization when spheroid-derived cells were treated with the mixture of OIM and BMP-2. These findings indicate that compared with monolayer MSCs, spheroid-derived MSCs are more susceptible to BMP-2, resulting in an acceleration of osteogenic differentiation at both early and late stages.

Our data indicate that BMP-2 enhances expression of osteogenic factors in spheroid-derived MSCs, therefore, we investigated the expression of Runx2. Runx2 is a master transcription factor, and both endochondral and intramembranous bone formation are inhibited in Runx2-null mice[28]. BMPs and Runx-2 cooperatively interact to stimulate osteoblast gene expression[29], and Runx-2 is essential for BMPs signaling in osteoblast differentiation[28]. In addition, Runx-2 is required for osteoblastic differentiation and bone formation during embryonic development[30, 31]. In this study, *Runx-2* mRNA expression was upregulated in spheroid-derived MSCs treated with the mixture of OIM and BMP-2. Similarly, OSX, a zinc-finger-containing transcription factor, is required for osteoblast differentiation and bone formation. OSX-null preosteoblasts are blocked from differentiating into mature osteoblasts and express chondrogenic markers and can differentiate into both chondrocytes and osteoblasts[32], indicating that OSX is necessary for mature bone formation. Our results showed increased expression of both Runx-2 and OSX in spheroid-derived MSCs cultured in the mixture of OIM and BMP-2. Furthermore, addition of BMP-2 enhanced intranuclear expression of OSX in spheroid-derived MSCs, indicating promotion of transcriptional activity or osteogenic differentiation.

The BMP and Wnt families are essential for commitment and differentiation of the osteoblast lineage[33] and BMPs play significant roles in bone formation via Smad-dependent pathways[34]. In this study, we demonstrate that spheroid-derived MSCs exhibited upregulation of *Smad5* mRNA and increased pSmad 1/5 expression. BMPs induces canonical Smad 1/5/8 phosphorylation[35] and it has been postulated that Smad 1/5/8 are intracellular signaling proteins that transduce signals elicited by members of the BMP signaling pathway in osteoblasts. Following BMP induction, Smad pathways converge at the *Runx2* gene to control mesenchymal precursor cell differentiation. The coordinated activity of Smads activated by Runx2 and BMP is critical for bone formation[34]. Additionally, OSX is indispensable for bone formation as it is required for differentiate of preosteoblasts into mature osteoblasts[36]. Increased expression of OSX induced by BMP-2 treatment is mediated by distal-less homeboy 5 (Dxl5), an essential regulator of BMP-2-induced osteoblast differentiation and a bone-inducing homeodomain transcription factor expressed in the latter stages of osteoblast differentiation[37]. Therefore, Dxl5 may directly interact with OSX[8]. From these reports, we suggest that increased expression of both Runx2 and OSX is regulated by a Smad-dependent BMP pathway in spheroid-derived MSCs.

β-catenin is a transcription regulator in the canonical Wnt signaling pathway, which has several functions in osteoblastogenesis[22]. BMP-2 and β-catenin synergize to promote osteoblast differentiation by stimulating ALP activity during osteogenic differentiation of multipotent embryonic cell lines which partially relies on Wnt signaling, suggesting that β-catenin may regulate osteoblastic differentiation via multiple mechanisms[38]. However, in our experiments using spheroid-derived MSCs, BMP-2 stimulation did not enhance expression of β-catenin. Therefore, in spheroid-derived MSCs originating from human adipose tissues, enhancement of osteogenic differentiation by BMP-2 is independent of the canonical Wnt signaling pathway, which is supported by previous studies[39].

There are three possible limitations in our study. First, our study may be limited by the lack of direct evidence to define why spheroid-derived MSCs are susceptible to BMP-2 treatment, compared with MSCs in monolayer culture. Spheroid formation is regulated by integrin-extracellular matrix (ECM) and cadherin-cadherin interactions[40, 41]. Recent studies proposed that integrins are found to enhance BMP-2 receptor activity and induce smad phosphorylation via Cdc42-Src-FAK-ILK pathway[42, 43]. Therefore, we speculate that spheroid-derived MSCs may maintain enhancement of integrin activity. Secondly, although recent studies have suggested that cross-talk between BMP-2 and Wnt signaling pathway promotes osteogenesis in MSCs[39], BMP-2 treatment did not induce noncanonical Wnt signaling pathway in spheroid-derived MSCs as evidence by no change in β-catenin expression. Induction of the noncanonical Wnt signaling pathway by BMP-2 treatment remains unclear. Therefore, further studies are warranted to examine the mechanisms of cross-talk between BMP-2 and Wnt signaling pathway in spheroid-derived MSCs during the osteogenesis. Finally, this study may be limited by the lack of direct evidence to elucidate whether spheroid-derived MSCs treated with BMP-2 can accelerate bone formation *in vivo*. However, we expect that an implantation of BMP-2-stimulated spheroid-derived MSCs can promote bone regeneration in an *in vivo* bone defect model based on evidence of enhanced calcium deposition *in vitro*.

In conclusion, this study revealed that spheroid-derived MSCs treated with BMP-2 exhibit enhanced osteogenic differentiation via the canonical Smad-dependent BMP signaling pathway, which may be targeted to advance the osteogenesis capacity of MSCs and provide unique strategies for bone regeneration and repair.

Acknowledgements

We would like to thank Enago (www.enago,jp) for the English language review. This work was supported by JSPS KAKENHI (Grant Number: 18K09567 to JO) and Private University Research Branding Project.

Conflict of Interest

The authors declare that they have no competing interest.

References

1. Pittenger MF, Mackay AM, Beck SC, Jaiswal RK, Douglas R, Mosca JD, Moorman MA, Simonetti DW, Craig S and Marshak DR. Multilineage potential of adult human mesenchymal stem cells. Science 284: 143-147, 1999
2. Zuk PA. Stem cell research has only just begun. Science 293: 211-212, 2001
3. Sudo K, Kanno M, Miharada K, Ogawa S, Hiroyama T, Saijo K and Nakamura Y. Mesenchymal progenitors able to differentiate into osteogenic, chondrogenic, and/or adipogenic cells in vitro are present in most primary fibroblast-like cell populations. Stem Cells 25:

1610-1617, 2007
4. Caplan AI. Adult mesenchymal stem cells for tissue engineering versus regenerative medicine. J Cell Physiol 213: 341-347, 2007
5. Blum JS, Barry MA, Mikos AG and Jansen JA. In vivo evaluation of gene therapy vectors in ex vivo-derived marrow stromal cells for bone regeneration in a rat critical-size calvarial defect model. Hum Gene Ther 14: 1689-1701, 2003
6. Osugi M, Katagiri W, Yoshimi R, Inukai T, Hibi H and Ueda M. Conditioned media from mesenchymal stem cells enhanced bone regeneration in rat calvarial bone defects. Tissue Eng Part A 18: 1479-1489, 2012
7. Canalis E, Economides AN and Gazzerro E. Bone morphogenetic proteins, their antagonists, and the skeleton. Endocr Rev 24: 218-235, 2003
8. Lee MH, Kwon TG, Park HS, Wozney JM and Ryoo HM. BMP-2-induced Osterix expression is mediated by Dlx5 but is independent of Runx2. Biochem Biophys Res Commun 309: 689-694, 2003
9. Cheng H, Jiang W, Phillips FM, Haydon RC, Peng Y, Zhou L, Luu HH, An N, Breyer B, Vanichakam P, Szatkowski JP, Park JY and He TC. Osteogenic activity of the fourteen types of human bone morphogenetic proteins (BMPs). J Bone Joint Surg Am 85-A: 1544-1552, 2003
10. Baraniak PR and McDevitt TC. Scaffold-free culture of mesenchymal stem cell spheroids in suspension preserves multilineage potential. Cell Tissue Res 347: 701-711, 2012
11. Zuk PA, Zhu M, Mizuno H, Huang J, Futrell JW, Katz AJ, Benhaim P, Lorenz HP and Hedrick MH. Multilineage cells from human adipose tissue: implications for cell-based therapies. Tissue Eng 7: 211-228, 2001
12. Huang GS, Tseng CS, Linju Yen B, Dai LG, Hsieh PS and Hsu SH. Solid freeform-fabricated scaffolds designed to carry multicellular mesenchymal stem cell spheroids for cartilage regeneration. Eur Cell Mater 26: 179-194, 2013
13. Bhang SH, Cho SW, La WG, Lee TJ, Yang HS, Sun AY, Baek SH, Rhie JW and Kim BS. Angiogenesis in ischemic tissue produced by spheroid grafting of human adipose-derived stromal cells. Biomaterials 32: 2734-2747, 2011
14. Potapova IA, Gaudette GR, Brink PR, Robinson RB, Rosen MR, Cohen IS and Doronin SV. Mesenchymal stem cells support migration, extracellular matrix invasion, proliferation, and survival of endothelial cells in vitro. Stem Cells 25: 1761-1768, 2007
15. Su G, Zhao Y, Wei J, Han J, Chen L, Xiao Z, Chen B and Dai J. The effect of forced growth of cells into 3D spheres using low attachment surfaces on the acquisition of stemness properties. Biomaterials 34: 3215-3122, 2013
16. Wang W, Itaka K, Ohba S, Nishiyama N, Chung UI, Yamasaki Y and Kataoka K. 3D spheroid culture system on micropatterned substrates for improved differentiation efficiency of multipotent mesenchymal stem cells. Biomaterials 30: 2705-2715, 2009
17. Hsu SH, Huang GS, Lin SY, Feng F, Ho TT and Liao YC. Enhanced chondrogenic differentiation potential of human gingival fibroblasts by spheroid formation on chitosan membranes. Tissue Eng Part A 18: 67-79, 2012
18. Huang GS, Dai LG, Yen BL and Hsu SH. Spheroid formation of mesenchymal stem cells on chitosan and chitosan-hyaluronan membranes. Biomaterials 32: 6929-6945, 2011
19. Yamaguchi Y, Ohno J, Sato A, Kido H and Fukushima T. Mesenchymal stem cell spheroids exhibit enhanced in-vitro and in-vivo osteoregenerative potential. BMC Biotechnol 14: 105, 2014
20. Toda M, Ohno J, Shinozaki Y, Ozaki M and Fukushima T. Osteogenic potential for replacing cells in rat cranial defects implanted with a DNA/protamine complex paste. Bone 67: 237-245, 2014
21. Sato A, Kajiya H, Mori N, Sato H, Fukushima T, Kido H and Ohno J. Salmon DNA Accelerates Bone Regeneration by Inducing Osteoblast Migration. PLoS One 12: e0169522, 2017
22. MacDonald BT, Tamai K and He X. Wnt/beta-catenin signaling: components, mechanisms, and diseases. Developmental cell 17: 9-26, 2009
23. Kapur SK, Wang X, Shang H, Yun S, Li X, Feng G, Khurgel M and Katz AJ. Human adipose stem cells maintain proliferative, synthetic and multipotential properties when suspension cultured as self-assembling spheroids. Biofabrication 4: 025004, 2012
24. Vinci M, Gowan S, Boxall F, Patterson L, Zimmermann M, Court W, Lomas C, Mendiola M, Hardisson D and Eccles SA. Advances in establishment and analysis of three-dimensional tumor spheroid-based functional assays for target validation and drug evaluation. BMC Biol 10: 29, 2012
25. Cheng SL, Yang JW, Rifas L, Zhang SF and Avioli LV. Differentiation of human bone marrow osteogenic stromal cells in vitro: induction of the osteoblast phenotype by dexamethasone. Endocrinology 134: 277-286, 1994
26. Kaartinen MT, El-Maadawy S, Rasanen NH and McKee MD. Tissue transglutaminase and its substrates in bone. J Bone Miner Res 17: 2161-2173, 2002
27. Maniatopoulos C, Sodek J and Melcher AH. Bone formation in vitro by stromal cells obtained from bone marrow of young adult rats. Cell Tissue Res 254: 317-330, 1988
28. Javed A, Afzal F, Bae JS, Gutierrez S, Zaidi K, Pratap J, van Wijnen Aj, Stein JL, Stein GS and Lian JB. Specific residues of RUNX2 are obligatory for formation of BMP2-induced RUNX2-SMAD complex to promote osteoblast differentiation. Cells Tissues Organs 189: 133-137, 2009
29. Phimphilai M, Zhao Z, Boules H, Roca H and Franceschi RT. BMP signaling is required for RUNX2-dependent induction of the osteoblast phenotype. J Bone Miner Res21: 637-646, 2006
30. Hassan MQ, Tare RS, Lee SH, Mandeville M, Morasso MI, Javed A, van Wijnen AJ, Stein JL, Stein GS and Lian JB. BMP2 commitment to the osteogenic lineage involves activation of Runx2 by DLX3 and a homeodomain transcriptional network. J Biol Chem 281: 40515-40526, 2006
31. Yang F, Yuan PW, Hao YQ and Lu ZM. Emodin enhances osteogenesis and inhibits adipogenesis. BMC Compl Altern Med 14: 74, 2014
32. Nakashima K, Zhou X, Kunkel G, Zhang Z, Deng JM, Behringer RR and de Crombrugghe B. The novel zinc finger-containing transcription factor osterix is required for osteoblast differentiation and bone formation. Cell 108: 17-29, 2002
33. Benarroch EE. Suprachiasmatic nucleus and melatonin: reciprocal interactions and clinical correlations. Neurology 71: 594-598, 2008
34. Chen G, Deng C and Li YP. TGF-beta and BMP signaling in osteoblast differentiation and bone formation. Int J Biol Sci 8: 272-288, 2012
35. Zhou Z, Xie J, Lee D, Liu Y, Jung J, Zhou L, Xiong S, Mei L and Xinog WC. Neogenin regulation of BMP-induced canonical Smad signaling and endochondral bone formation. Dev Cell 19: 90-102, 2010
36. Zhang C. Transcriptional regulation of bone formation by the osteoblast-specific transcription factor Osx. J Orthop Surg Res 5: 37,

2010
37. Ryoo HM, Hoffmann HM, Beumer T, Frenkel B, Towler DA, Stein GS, Stein JL, van Wijnen AJ and Lian JB. Stage-specific expression of Dlx-5 during osteoblast differentiation: involvement in regulation of osteocalcin gene expression. Mol Endocrinol 11: 1681-1694, 1997
38. Rawadi G, Vayssiere B, Dunn F, Baron R and Roman-Roman S. BMP-2 controls alkaline phosphatase expression and osteoblast mineralization by a Wnt autocrine loop. J Bone Miner Res18: 1842-1853, 2003
39. Nakashima A, Katagiri T and Tamura M. Cross-talk between Wnt and bone morphogenetic protein 2 (BMP-2) signaling in differentiation pathway of C2C12 myoblasts. J Biol Chem 280: 37660-37668, 2005
40. Salmenpera P, Kankuri E, Bizik J, Siren V, Virtanen I, Takahashi S, Leiss M, Fassler R and Vaheri A. Formation and activation of fibroblast spheroids depend on fibronectin-integrin interaction. Exp Cell Res 314: 3444-3452, 2008.
41. Cui X, Hartanto Y and Zhang H. Advances in multicellular spheroids formation. J R Soc Interface 14: 20160877, 2017.
42. Ashe HL. Modulation of BMP signalling by integrins. Biochem Soc Trans 44: 1465-1473, 2016.
43. Fourel L, Valat A, Faurobert E, Guillot R, Bourrin-Raynard I, Ren K, Lafacnechere L, PLanus E, Picart C and Albiges-Rizo C. b3 integrin-mediated spreading induced by matrix-bound BMP-2 controls smad signaling in a stiffness-independent manner. J Cell Biol 212: 693-706, 2016.